Chemical Papers (2021) 75:6487–6497
https://doi.org/10.1007/s11696-021-01815-4

ORIGINAL PAPER

Metal doped fullerene complexes as promising drug delivery materials against COVID-19

Shamsa Bibi[1] · Shafiq Urrehman[1] · Laryeb Khalid[1] · Muhammad Yaseen[2] · Abdul Quyyam Khan[3] · Ran Jia[4]

Received: 21 May 2021 / Accepted: 2 August 2021 / Published online: 9 August 2021

Abstract

An outbreak of respiratory disorder caused by coronavirus has been named as coronavirus infection 2019 (COVID-19). To find a specific treatment against this disease researchers are at the frontline. To cure COVID-19, favipiravir (FPV) has been reported as an effective drug based on its high recovery rate. Among nanomaterials, fullerene C60 has achieved enormous attention as a drug delivery vehicle due to its good bioavailability and low toxicity. Hence, in this work, we have investigated the potential of metal-doped fullerene as a drug carrier, based on DFT calculations by using M06-2X functional and 6-31G(d) basis set in water media. In this research electronic parameters and adsorption energy of FPV on interaction with metal-doped (Cr, Fe, and Ni) fullerene is studied. The charge transfer between drug and doped fullerene has been studied through electrophilicity indexes. The structural and electronic properties are explored in terms of adsorption energy through frontier molecular orbital (FMO) and density of state (DOS). It is observed that doping of fullerene C60 with Cr, Fe, and Ni metals significantly enhances the drug delivery rate and provides numerous advantages including controlled drug release at specific target sites which minimize the generic collection in vivo and reduce the side effects. Thusly, it is suggested that our designed metal-doped complexes might be efficient candidates as drug delivery materials for COVID-19 infection.

Graphic abstract

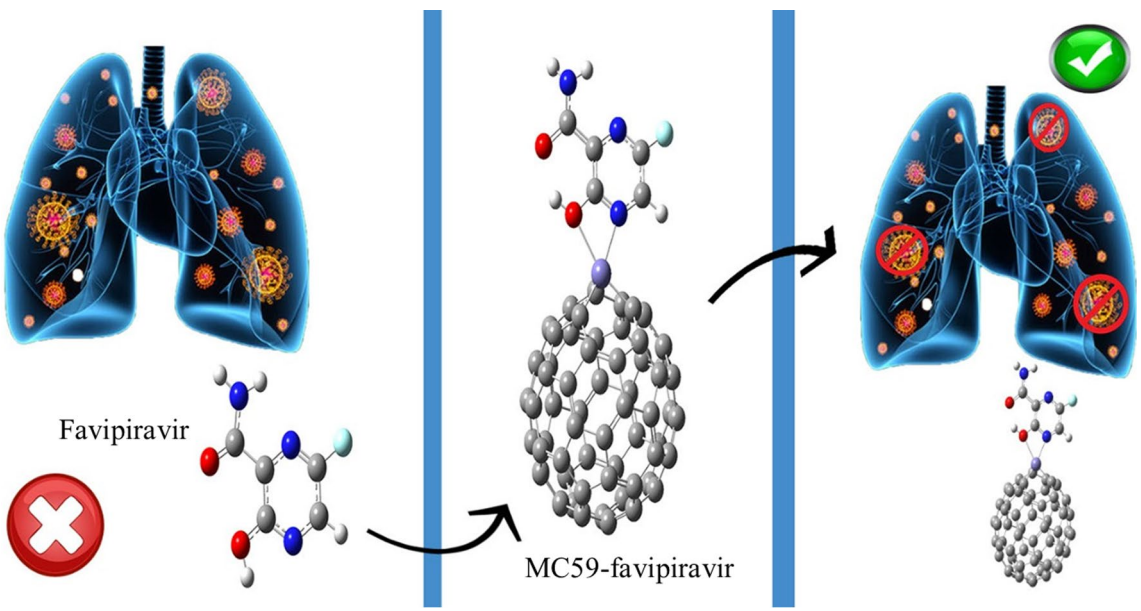

Keywords Density functional theory · Doping · COVID-19 · Fullerene · Metal-complexes · Drug delivery

Extended author information available on the last page of the article

Introduction

In December 2019, the first case of coronavirus known as coronavirus infection 2019 (COVID-19) similar to severe acute respiratory syndrome (SARS) was reported in China and spread across the globe within two months (Zu et al. 2020). It is a respiratory disorder and has become the major pathogen of emergency respiratory outbreaks (Harapan et al. 2020). According to the latest studies, the most common symptoms of coronavirus illness are fever, dry cough, fatigue, myalgia, and the less common symptoms are abdominal pain, headache, nausea, vomiting, and diarrhoea (Song et al. 2020). Often infected patients of coronavirus lead to multiple organ failure due to severe respiratory disorder that results in a high mortality rate (Liu et al. 2020). The SARS was started about 18 years ago, genetically indistinguishable and having 79.6% uniqueness with COVID-19. This similarity can be advantageous for theoretical investigation (Hiscott et al. 2020). However, to control the spread of this disease and to discover an effective antiviral drug, the healthcare workforces are in the research battle zone (Huang et al. 2020).

For the treatment of coronavirus different antiviral drugs, including Remdesivir, Favipiravir, Arbidol, and Chloroquine are under investigation (Dong et al. 2020; Wu et al. 2020). Comparison between Remdesivir and Favipiravir (FPV) suggests that FPV can be most effective to cure coronavirus based on its high recovery rate and reduce the pyrexia and cough (Sreekanth Reddy and Lai 2021). FPV is an RNA-dependent RNA polymerase (RdRp) inhibitor that is effective for the treatment of the Ebola virus and influenza (Sissoko et al. 2016). Recently it has been highlighted that FPV as a prodrug was efficacious in reducing coronavirus infection (Udwadia et al. 2021). So clinical researchers are required to check the effectiveness and safety of this antiviral drug against coronavirus.

In pharmaceuticals, nanostructure-based drug delivery system has become most efficient to reduce side effects and improve the bioavailability of the drug. In comparison with conventional dosage, these drug delivery systems provide numerous advantages including controlled drug release at the specific effective site, minimize generic collection in vivo tissues, enhance cellular uptake, improve adsorption and reduce the harmful side effect of drugs (Slepička et al. 2013; Parlak and Alver 2017). Various nanostructures have been established for drug delivery applications which are superior to microstructures because of the high surface to volume ratio. Among nanomaterial carbon-based nanomaterials including graphene, fullerene, and carbon nanotubes (CNT) have been widely considered because of their unique physical and chemical properties in nanotechnology as drug delivery vehicles (Raphey et al. 2019). A drug delivery system is considered a major therapy, as it employs nanomaterials to deliver a specific amount of drug at the targeted site in a controlled way (Hazrati and Hadipour 2016a, b). Nanostructures help to load and conjugate the drug molecule to the targeted cells so can be used as an ideal candidate for drug delivery.

Among nanomaterials, fullerene and its derivatives have achieved enormous attention to use as drug delivery purposes due to their unique properties such as hollow cage-like structure, versatile physical, chemical, and biological properties, effective drug loading capability, and antioxidant capacity (Hazrati and Hadipour 2016a, b; Ergürhan et al. 2018). On the other hand, also having fewer biological side effects due to its hydrophilicity. As carbon is hydrophobic, so the major limitation of carbon-based nanomaterials for biological application is their hydrophobicity (Kazemzadeh and Mozafari 2019). To overcome this problem various methods such as surface functionalization with specific groups, encapsulation, and chemical modification through doping by using specific atoms are commonly used to show promising results and to enhance the hydrophilicity of nanostructures (Kumar and Raza 2017; Henna et al. 2020; Maleki et al. 2020). It is also investigated that through the doping phenomenon adsorption properties and sensitivity can be improved. Magnetic and electronic properties can also be improved through doping and functionalization to get the desired results (Parlak et al. 2020).

Different theoretical and experimental studies have been done to investigate the interaction between different drugs and fullerene (Bashiri et al. 2017; Samanta and Das 2017; Parlak et al. 2020). It has been concluded that doping of fullerene with metal is suitable to improve the drug delivery system through enhancing adsorption potential (Hazrati and Hadipour 2016a, b). It also has been investigated from previous work that Ni and Cr doped fullerene significantly improves the adsorption of uracil, thymine and adenine (Rad and Aghaei 2018). In this work, we aimed to check the ability of fullerene as a favourable candidate of drug delivery to adsorb FPV drugs through density functional theory (DFT) calculations. Recently a theoretical study was carried out to investigate adsorption between doped and undoped fullerene and FPV. In which nine different possible interactions were checked. It was observed that -N,-OH, and -OH interaction edges have the highest adsorption energy in the water phase (Parlak et al. 2017). In another study, it was also investigated the adsorption between transition metal-doped C20 and FPV (Rad et al. 2020).

Notably, there is no work on the interaction between -N, -OH interaction edges of FPV and chromium (Cr), iron (Fe), and nickel (Ni) doped C60. Therefore, in the following research, we are going to design FPV…CrC59, FPV…FeC59, and FPV…NiC59 complexes, to investigate adsorption energy between FPV and iron (Fe), chromium (Cr), and

nickel (Ni) doped C60 for the first time (Scheme 1). The experimental investigation on new material is also essential but they are time-consuming and costly and do not give enough information. Therefore, computational work has been employed to understand the nature of interaction and its mechanism (Hazrati and Hadipour 2016a, b; Novir and Aram 2020). Some of the important chemical properties such as binding energy (E_b), energy gap (E_g), electrophilicity indexes (ω), chemical hardness (η), the electronegativity of a system (χ), and maximum electronic charge (ΔN_{max}), density of states (DOS) and molecular electrostatic potential maps (MEPS) have been calculated in this work.

Computational details

All calculations were carried out with Gaussian 09 program (Shi et al. 2010). Initially, all the structures of complexes were built through the GaussView program 6.0 (Dikmen et al. 2018). To get the most stable configuration, optimization of all structures was computed by density functional theory (DFT) method with M06-2X functional and 6-31G(d) basis set (Patel and Singh, 2018). PyMOlyze 2.0 program was used to calculate the density of state (DOS).

To define the relative stability regarding the nanostructures-drug interactions of complexes adsorption or binding energy has been performed through the following equation.

$$E_{ads} = E_{complex} - E_{C59} - E_{FPV} \quad (1)$$

In Eq. (1), $E_{complex}$ is the total energy of doped fullerene attached with drug, $E_{C59,}$ and E_{FPV} is individual energies of optimized structures. The counterpoise (cp) correction method is used to eliminate the basis set superposition error (BSSE) (Boys and Bernardi 2006).

The effect of FPV adsorption on electronic parameters has been investigated through the energy gap (E_g). E_g is the difference between the highest occupied molecular orbital (HOMO) and lowest unoccupied molecular orbital (LUMO). To measure stabilization energy, the electrophilicity index (ω) is one of the focal parameters when a system gets an additional electronic charge. Electrophilicity index is a charge transfer descriptor and calculated by the following equation (Korotkikh et al. 2019).

$$\mu = \left(E_{HOMO} + E_{LUMO}\right)/2 \quad (2)$$

$$\eta = \left[-E_{HOMO} - \left(-E_{LUMO}\right)\right]/2 \quad (3)$$

$$\omega = \mu^2/2\eta \quad (4)$$

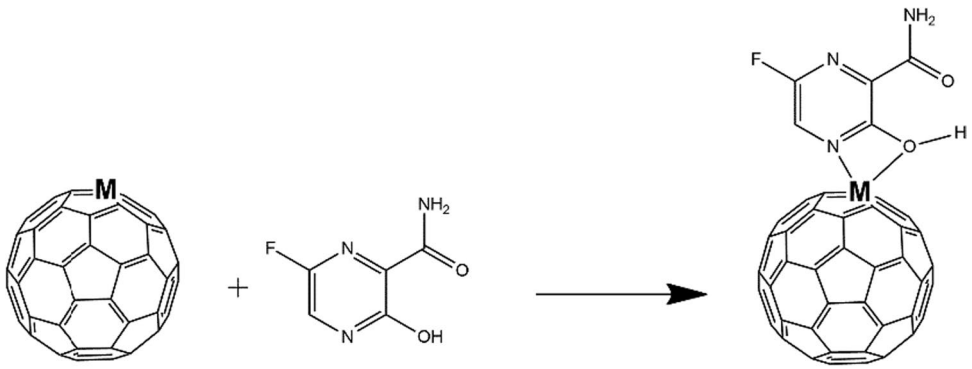

If

M = Cr **FPV...CrC59**

M = Fe **FPV...FeC59**

M = Ni **FPV...NiC59**

Scheme 1 Scheme of designed metal-doped complexes, FPV…CrC59, FPV…FeC59, and FPV…NiC59

In the above equations, μ and Ƞ represent the chemical potential and chemical hardness, respectively. The (ΔN_{max}), maximum electronic charge accepted from the surrounding have been calculated through the following formula.

$$\Delta N_{\max} = -\mu/\eta \tag{5}$$

$$\Delta N_{\max} = 2\omega/\chi \tag{6}$$

where χ is the electronegativity of the system and ω is the electrophilic index. The amount of charge transfer between drug and doped fullerene can be defined through electrophilicity.

$$\mathrm{ECT} = 2\left[\omega_{\mathrm{A}}\chi_A - \omega_{\mathrm{B}} - \chi_{\mathrm{B}}\right] \tag{7}$$

In the above equation χ_A is electronegativity of drug molecule and χ_B is electronegativity of doped fullerene, if ECT < 0 drug will act as donor, and if ECT > 0 drug will act as acceptor. To calculate the electronic sensitivity and to correlate it with electrical conductivity and energy gap following expression is used;

$$\sigma \propto \exp(-E_g/2kT) \tag{8}$$

In the above equation, k represents the Boltsman constant and an exponential relationship present between electrical conductivity and Eg.

Molecular electrostatic potential (ESP) has also been calculated by using the same basis set to investigate the nature of interaction and to study the charge distribution.

Results and discussion

Optimized structure

Due to the absence of charge distribution, C60 exhibits zero dipole moment. Through doping one of the carbon atoms from the C60 cage-like structure has been replaced by Cr, Fe, and Ni, and the final complexes have been optimized with the same M06-2X/6-31G(d) method in water media. The optimized structures of FPV…Cr59, FPV…FeC59, and FPV…NiC59 is presented in Fig. 1. According to the atomic charges, active sites of FeC59, CrC59, and NiC59 are Fe,

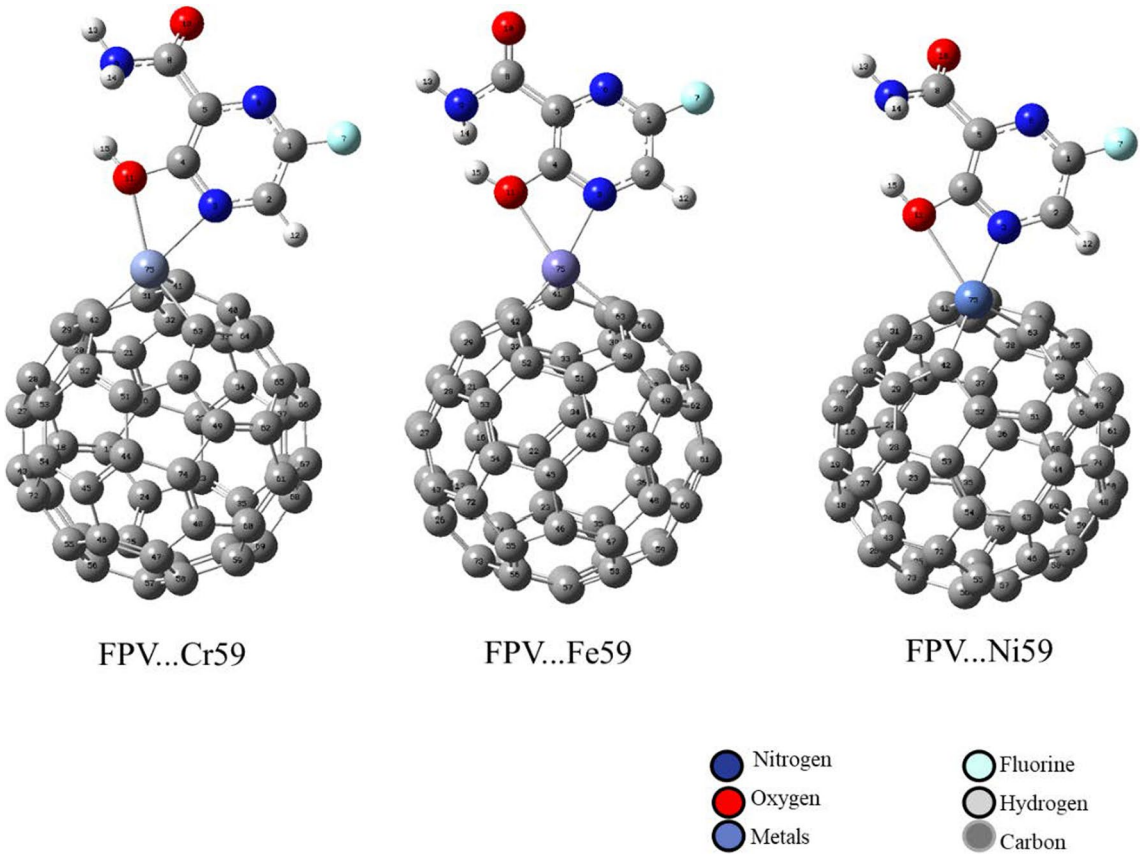

Fig. 1 Ground-state optimized structures of FPV…Cr59, FPV…FeC59, and FPV…NiC59 calculated at the level M06-2X/6-31G(d) of theory

Table 1 The calculated values of bond length, bond angle, and dihedral angle of designed FPV…Cr59, FPV…FeC59 and FPV…NiC59 complexes

Bond length (Å)	FPV…Cr59	FPV…FeC59	FPV…NiC59
M75-N3	2.257	2.128	2.071
M75-O11	2.284	2.262	2.883
M75-C63	1.968	1.884	1.869
M75-C41	1.942	1.881	1.868
M75-C42	1.847	1.782	1.833
C40-C41	1.463	1.459	1.436
C63-C50	1.385	1.389	1.373
C42-C52	1.473	1.468	1.451
C64-C65	1.399	1.399	1.395
N3-C2	1.324	1.323	1.333
C4-O11	1.353	1.348	1.331
C71-C70	1.388	1.388	1.388
C59-C60	1.449	1.448	1.448
Bond angle (°)			
N3-M75-C41	92.79	94.38	96.066
O11-M75-C42	120.75	107.25	124.359
N3-M75-C63	93.29	101.63	96.073
O11-M75-C41	110.34	97.55	79.49
Dihedral angle (°)			
C4-O11-M75-C42	− 173.73	− 178.89	167.32
C4-N3-M75-C63	− 174.55	− 176.17	150.34

Cr, and Ni, respectively, due to the distribution of positive charge around the metal atom. All the dopant atoms cause deformation in fullerene at the doped points. For numerical evaluation distance between different atoms of drug and metal-doped fullerene bond lengths is reported in Table 1. Bond angles and dihedral angles also have been calculated to study structural changes.

Table 1 indicates that doping of Fe, Cr, and Ni increases the distance of dopant atoms with other atoms, due to which deformation in a structure occurs and this deformation is more prominent for large size dopant atoms. The calculated bond lengths suggest that the interaction of FPV drug with metal-doped fullerene is considerable. It can be visualized that for each metal atom FPV had a unique configuration and orientation due to the hybridization of different orbital between them. Overall, it proves planner confirmation for all doped metal complexes.

It can be visualized from the results given in Table1 that slight variation in bond length and dihedral angle occur after the substitution of one of the carbon atoms with a metal atom. Among metal atoms, the Ni atom is more closely bonded with surrounding carbon atoms with a bond length of 1.869, 1.868, and 1.833. Also, the drug molecule is most strongly bound onto NiC59 with a bond length of 2.071. Hence, the highest adsorption energy was observed for the Ni atom making it the most stable adsorbent for FPV drug than others. Furthermore, the torsion angle expresses the rotatable bond conformation around their axis of rotation. The negative values of the dihedral angle express the anticlockwise, while positive values express the clockwise rotations. This study shows the electron flow from the drug (donor) to metal-doped fullerenes (acceptor) with less steric hindrance and great convenience. However, these results verified that metal doping may affect the geometrical parameters, but any drastic effect to distort the geometry and stability of the compound was not observed.

Adsorption of a drug on doped fullerenes (C59)

Through doping of electropositive metals, charge distribution occurs which results in increased dipole moment, electrophilicity, and more charge transfer from drug to fullerene which in turn increases the binding energy and decreases the E_g. After doping maximum charges are transferred to the doped electropositive metal atoms. So, these metal atoms are the active site for the binding energy of the drug. The negative values of binding energy indicate that adsorption of FPV with doped fullerene is an exothermic and spontaneous process (Table 2). Among all possible interaction edges of FPV to interact with doped fullerene, the most favourable edge is -N, -OH. On the other side, the dipole moment value increases after doping of metal, and charge density around the metal is maximized. Therefore, for fullerene, the metal atom is the most favourable site for energetic interaction. By comparison Cr, Fe and Ni, it can be visualized that, Ni-doped fullerene showed the highest binding energy towards

Table 2 Energetic, electronic and stability parameters of FPV drug, metal (Cr, Fe, Ni) doped fullerene and FPV…CrC59, FPV…FeC59, and FPV…NiC59 complexes

Molecules	Eg(eV)	μ(eV)	Ƞ(eV)	Ead(eV)	ω(eV)	ΔN_{max}	σ (eV)	ECT
FPV	7.10	− 5.09	3.55		3.64	1.43	0.28	
CrC59	4.10	− 4.36	2.05		4.64	2.17	0.48	
CrC59…FPV	4.08	− 4.35	2.04	− 1.96	4.44	2.22	0.49	− 2.70
FeC59	4.20	− 4.56	2.10		5.02	2.13	0.47	
FeC59…FPV	4.11	− 4.55	2.05	− 2.16	5.05	2.13	0.48	− 2.79
NiC59	3.71	− 4.86	1.86		6.34	2.61	0.53	
NiC59…FPV	3.48	− 4.16	1.74	− 9.08	4.97	2.39	0.57	− 2.96

drug, while the binding energy of Cr and Fe doped fullerenes are also considerable. These resulting binding energy values reveal that from moving left to right in the first row of transition metals E_g decreases and binding energy increases. Interestingly, it is also observed that a decrease in E_g and increase in binding energy for metal-doped C60 fullerene is more than that of C20 (Rad et al. 2020). Among all investigating compounds, FPV…NiC59 complex exhibits the highest binding energy and the strongest interaction in the water phase. Hence, results prove that the interaction of a drug with doped fullerene influencing the magnetic and electronic properties and this change is more prominent for Ni atom. Thus, doping of electropositive metals results in increased dipole moment which in turn enhances charge transfer from drug to fullerene with an increase in binding energy.

Frontier molecular orbital analysis (FMO)

The molecular structure of FPV and doped fullerene complexes were fully optimized in the ground state. Figure 2 displays that HOMO and LUMO energy levels were different for all complexes due to which changes in the electronic structure of doped metallofullerene were also different. It can be seen that HOMOs shifted to lower negative and LUMOs shifted to higher negative after the adsorption of the drug to the doped fullerene (Table S2). Biological activities also increase with an increase in E_{HOMO} or by a decrease in E_{LUMO}. Therefore, changes in E_g occur due to changes in HOMO and LUMO energy levels.

The irregular trend of HOMO and LUMO energy levels is due to doping of metals and this effect varies from metal to metal. The density distribution of HOMO and LUMO orbitals was also affected after the adsorption of the FPV drug on metallofullerenes (Fig. 3). For LUMO density distribution, the effect of drug adsorption was far obvious. In the case of

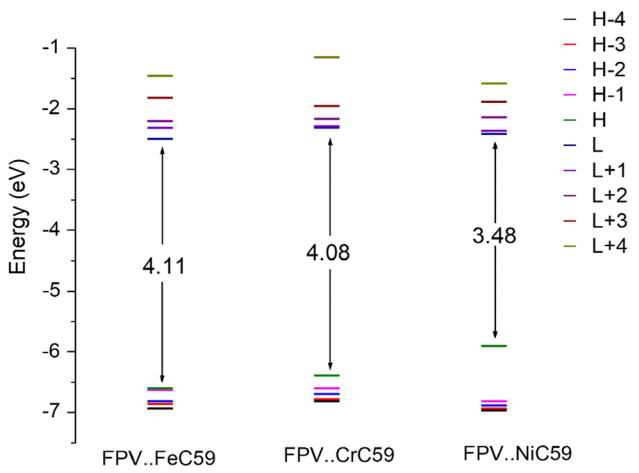

Fig. 2 Comparison of the Energy levels of three designed FPV…FeC59, FPV…CrC59 and FPV…NiC59 complexes

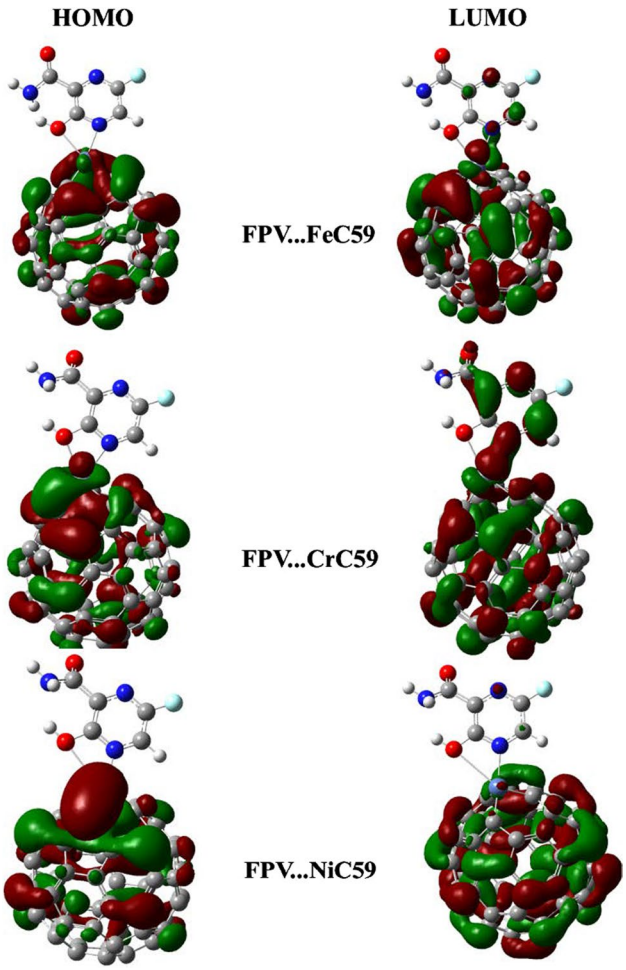

Fig. 3 HOMO and LUMO orbitals of optimized FPV…FeC59, FPV…CrC59 and FPV…NiC59 complexes

FPV…CrC59, LUMO orbital was almost shifted to the drug, while in the case of Fe and Ni complex this shift was also noticeable. This shift in the distribution of orbitals density occurs due to the transfer of charge from drug to metal atom. Graphical presentation of HOMO and LUMO along with E_g is provided in Fig. 2, Table S2.

As HOMO energy levels of all the complexes increases and LUMO energy levels decrease, E_g values for all complexes also decrease. From the obtained results, we can conclude that after the adsorption of FPV on the doped C60 E_g value decreases for FPV…FeC59, FPV…CrC59 and FPV…NiC59 complexes but this decrease in value is higher for Ni-doped C60. This means that the change in E_g for the configuration of Ni-doped fullerene interacting with FPV drug is more as compared to the Cr and Fe doped fullerene. Thus, we concluded that an electronically favourable interactions occur which change the FPV drug properties significantly.

The density of state (DOS)

This analysis gives a comparison of HOMO and LUMO energy levels of designed complexes and each constituent of a complex. Partial density of state (PDOS) shows the orbital distribution of individual component complex and total density of state (TDOS) shows the overall distribution of all orbitals in the complex. The change in E_g value in complexes after adsorption can be visualized. The DOS of each complex is given in Fig. 4, which reflects the change in height and displacement in their HOMO and LUMO levels. It can be estimated from the high relative intensity of drug and metal-doped complex that high conjugation results in high relative intensity. Observation of a change in DOS curves reflects the sensitivity of each complex which can be used to make an FPV drug a good electrochemical sensor.

Furthermore, mulliken analysis represents the %age contribution around the FMOs (Fig. 5, Table S1). The %age contribution of C59, FPV drug and Ni for HOMO is 65.7%, 11.2% and 23.1%, respectively, whereas C59 72.8%, FPV 17.9% and Ni 9.3% for LUMO. This contribution is also evident from DOS of FPV…NiC59. The %age composition of each building component in FPV…NiC59 is different for HOMO and LUMO. Likewise, C59, FPV drug and doped metal atom showed different %age contribution for HOMO and LUMOs in FPV…FeC59, FPV…CrC59 complexes. By comparing the %age contribution of all doped metals it can be visualized that contribution of Ni is higher for LUMO which results in efficient electronic transition (Table S1).

Electronic parameters

Electronic properties are vigorously correlated to the HOMO and LUMO, their energy values and distribution patterns. Therefore, our major focus is on a detailed investigation of E_g and the distribution pattern of FMOs.

To observe the electronic sensitivity and to correlate it with electrical conductivity and energy gap, values were calculated through Eq. 8. An exponential relationship is present between electrical conductivity and E_g. Compounds with

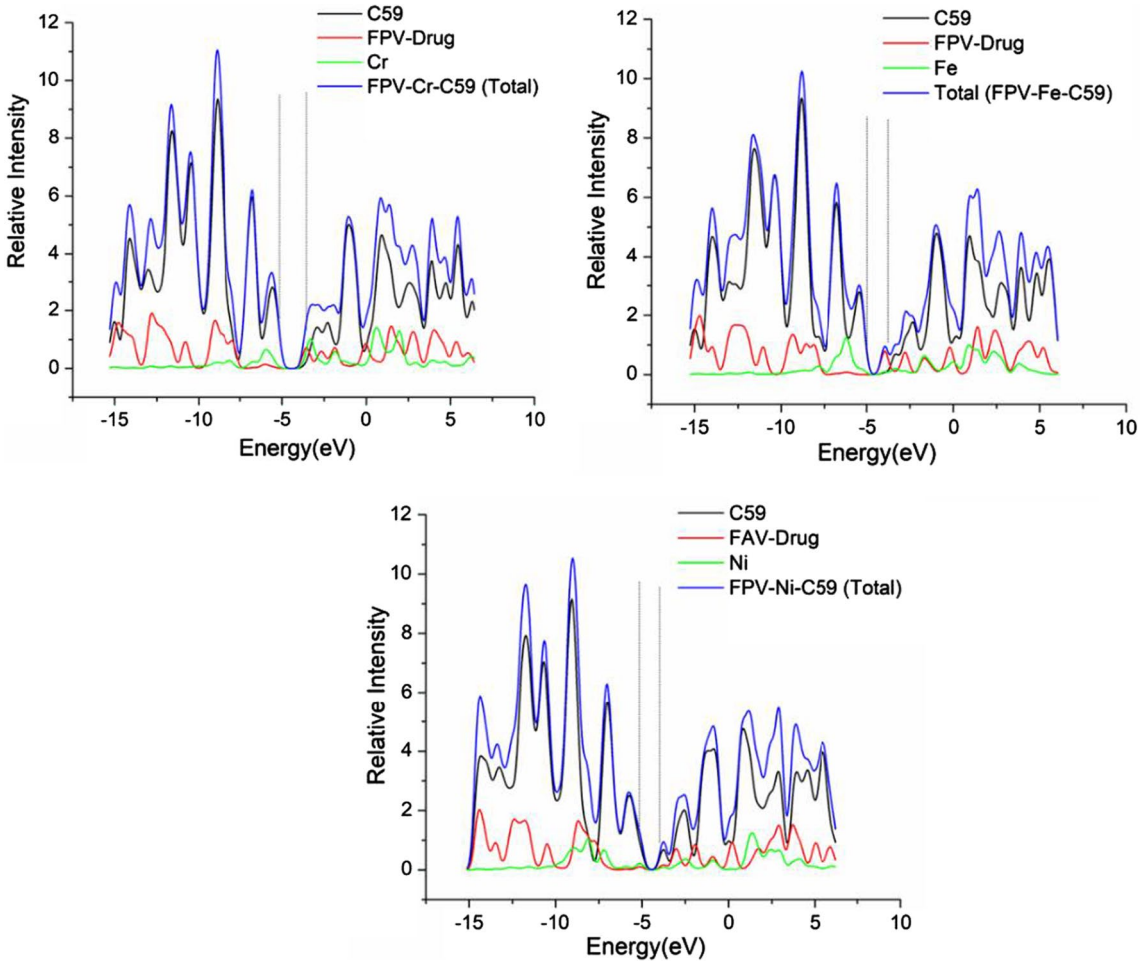

Fig. 4 PDOS and TDOS around HOMO and LUMO for designed FPV…CrC59, FPV…FeC59, and FPV…NiC59 complexes

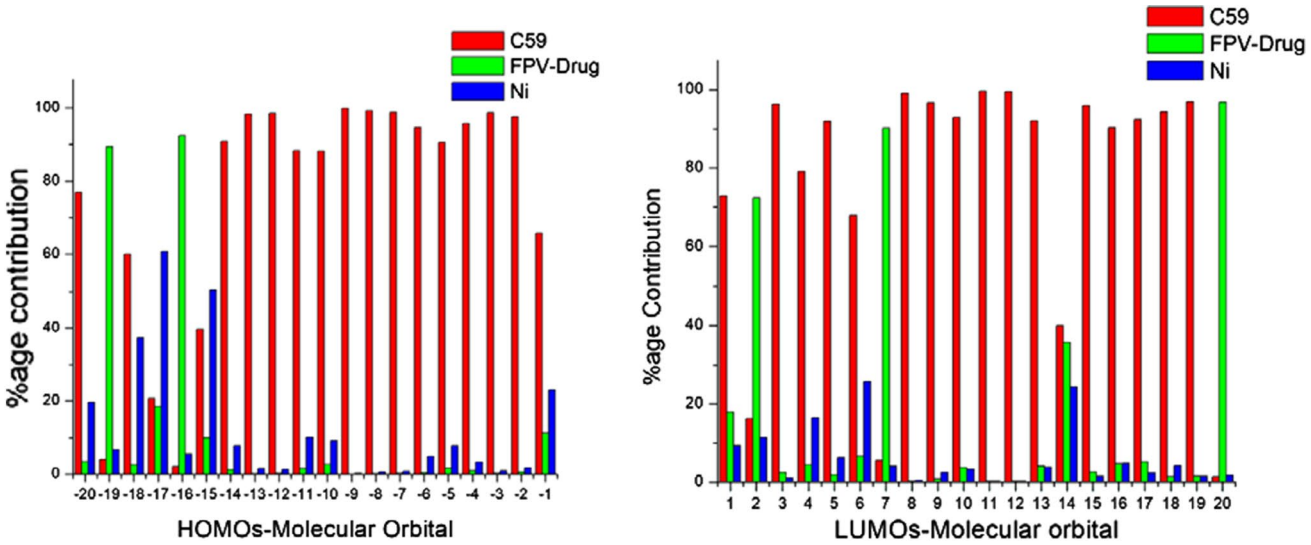

Fig. 5 Percentage contribution of each component in the FPV…NiC59 complex

less E_g value easily transfer electrons across the conduction band so the compounds with lower E_g value have higher electrical conductivity. It can be visualized from values listed in Table 2 that after adsorption of the drug to doped fullerene conductivity has been increased. The values of the electrophilic index and chemical reactivity were applied to estimate the reactivity and chemical stability of the compound. E_g plays a significant role in determining chemical stability. The polarizability, chemical hardness or softness, and reactivity are also calculated through formulas. To measure the reactivity of new molecules chemical hardness (Ƞ) is an important factor because molecules can easily alter their electronic density if they are structurally soft and biological activities are also higher for softer molecules. Moreover, for softer compounds, electronic transitions are better and easier which are essential for a chemical reaction. The values given in Table 2 show that after adsorption of FPV drug to metal doped C60 chemical hardness of complex molecule decreases as compared to FPV drug. Hence, doping of Cr, Fe and Ni causes a decrease in hardness. Therefore, a considerable decrease in hardness occurs for FPV…CrC59, FPV…FeC59, and FPV…NiC59 complexes. Thus, the comparison of all complexes indicates that complex FPV…NiC59 has greater softness so biologically more active and has higher adsorption power.

The electrophilicity (ω) and maximum electronic charge accepted from the environment (ΔN_{max}) are important factors for determining the tendency of a molecule to adsorb electrons. Whenever two molecules react one acts as a nucleophile and the others as an electrophile. The compounds with low electrophilicity can transfer electrons and the compounds with high electrophilicity can accept electrons. The electrophilicity of FPV drug after binding reduces which means that it has a lower capacity to accept electrons after adsorption.

The amount of charge transfer between drug and metallofullerene can also be explained through electrophilicity called electrophilicity-based charge transfer (ECT) can be calculated through the equation. The value of ECT indicates ECT < 0, so the drug behaves as a donor and the charge is transferred from drug to metal atom.

The dipole moment is another good parameter to measure the solubility of compounds in polar solvents. Therefore, compounds with higher dipole moments are highly soluble in water. According to results, dipole moment increases after adsorption of FPV drug with doped fullerene due to which polarity of complex increases (Table S3). Hence an increase in dipole moment is a favourable property to deliver the drug in the biological system. Based on calculated parameters, we conclude that after adsorption of the drug to fullerene Eg decreases for FPV…CrC59, FPV…FeC59, and FPV…NiC59 complexes due to which charge transfer from drug to fullerene increases, electrophilicity decreases and adsorption energy increases. Hence, this analysis indicates that complex of FPV drug with Ni-doped fullerene having the lowest Eg value than those of Cr and Fe doped complexes exhibits the highest adsorption energy.

Molecular electrostatic potential surfaces (MEPS)

Molecular electrostatic potential surfaces (MEPS) are an important parameter to explain the relationship of electrophile and nucleophile attachment points. MEPS have been calculated to understand the nature of nucleophilic and electrophilic attacking sites. MEPS drawn from the optimized structure are shown in Fig. 6. In MEPS, red and blue colours

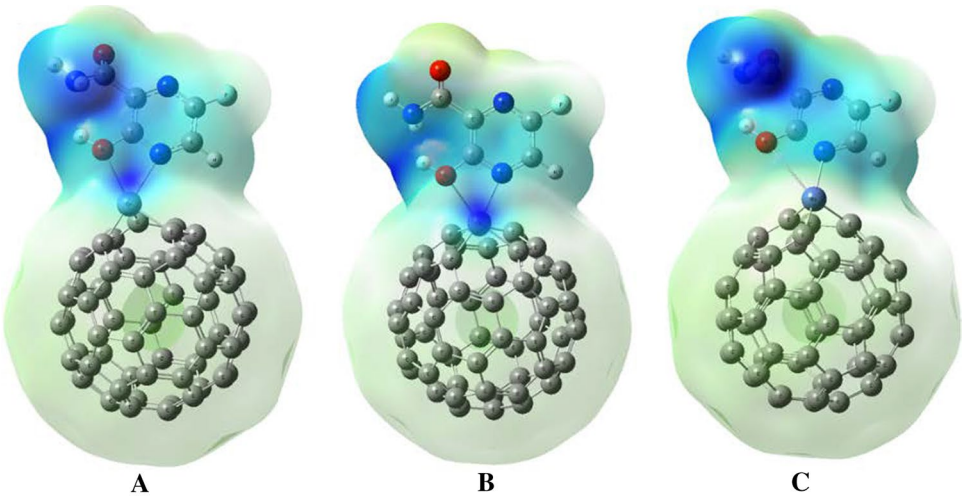

Fig. 6 Electrostatic potential maps of designed complexes A) FPV…CrC59 B) FPV…FeC59 C) FPV…NiC59

indicate the nucleophilic and electrophilic regions, respectively (Bibi et al. 2019). MEPS maps show that for nucleophilic attack positive region is more favourable and for an electrophile to attack the negative region is more favourable. Possible interaction sites of FPV and doped fullerene have been purposed through MEPS maps. By considering the previous research and considering the interaction edge of the drug, it can be estimated from MEPS of FPV and Cr, Fe, and Ni-doped fullerene that for a ligand to interact, Fe, Cr, and Ni metal atoms are considered as the most active site because of positive charge distribution around the metal. In water solvent, the strongest interaction occurs from the -N, -OH edge of the drug and this edge is energetically more favourable than others. One reason for the favourable geometry of this edge is that there is a possibility of two bond formation (Rad et al. 2021). The binding energy of FPV interacted with metal doped fullerene is given in Table 2. From binding energy, it can suggest that chemisorption occurs between drug and doped molecule. In chemisorption new chemical bond formation occurs between interacting molecules, therefore interatomic distance must be at a feasible length. Thus, it can be concluded that favourable interactions occur in FPV…CrC59, FPV…FeC59, and FPV…NiC59 complexes. So, these metal doped fullerenes might be an advantageous candidate for drug delivery. It can be visualized from binding energy and electrophilicity index values (Table 2) that among all metal atoms Ni doping significantly enhances the tendency of fullerene to adsorb FPV drug.

Conclusion

In this work, DFT calculations were carried out with M06-2X/6-31G(d) method to explore the interaction between FPV drug and three metal-doped fullerenes (CrC59, FeC59, NiC59) to investigate the final three complexes (FPV…CrC59, FPV…FeC59, and FPV…NiC59) as drug delivery materials for COVID-19 treatment. All the calculations were carried out using Gaussian09 in water media. Among various interaction edges of FPV drug, the -N, and -OH edges were used to study the binding energy and other electronic parameters. After the interaction of the drug to doped fullerene, HOMO shifted to lower negative and LUMO shifted to higher negative values, which resulted in a decrease Eg. The compounds with lower Eg easily transfer electrons across the conduction band which resulted in higher electronic properties. The most negative binding energy was observed for FPV…NiC59, it showed that there exists the strongest interaction between FPV drug and Ni-doped fullerene. The decrease in Eg proved that Cr, Fe, and Ni-doped complexes are electronically harmless and significantly alter the FPV drug properties. Among all complexes, FPV…NiC59 exhibited the highest value of conductivity. An increase in the electrophilic index (ω) of metal-doped fullerene complexes as compared to a pure drug indicated that drug after adsorption with doped fullerene showed more electrophilicity for the observed complexes. Similarly, values of electrophilic charge transfer (ECT) showed that doped C59 acts as electron acceptor and drug as the electron donor. After the adsorption of FPV drug with the metal-doped fullerene, dipole moment value was increased which is a favourable property for these complexes to be used as drug delivery vehicle in a biological system for the purpose of antiviral diseases. In addition, a decrease in Eg and increase in binding energy for metal doped C60 fullerene was more than that of previously studied C20 doped complexes. Hence, based on these results, we can conclude that Cr, Fe and particularly Ni doped fullerene can efficiently adsorb FPV drug and would be the best nano-drug delivery material in COVID-19 treatment due to improved electronic and enhanced adsorption properties.

Supplementary Information The online version contains supplementary material available at https://doi.org/10.1007/s11696-021-01815-4.

Acknowledgements The calculations were performed in the computational and theoretical chemistry laboratory at the department of chemistry, University of Agriculture Faisalabad, Faisalabad, Pakistan. The authors vastly acknowledge the Higher education commission (HEC) of Pakistan for financial support. The authors also acknowledge Institute of Theoretical Chemistry and College of Chemistry, Jilin University, Changchun, China for technical support.

References

Alver DGÖ, Parlak C (2018) NMR determination of solvent dependent behavior and XRD structural properties of 4-carboxy phenylboronic acid: a DFT supported study. Chem Phys Lett 698:114–119. https://doi.org/10.1016/j.cplett.2018.03.005

Bashiri S, Vessally E, Bekhradnia A, Hosseinian A, Edjlali L (2017) Utility of extrinsic [60] fullerenes as work function type sensors for amphetamine drug detection: DFT studies. Vacuum 136:156–162. https://doi.org/10.1016/j.vacuum.2016.12.003

Bibi S, Shafiqur R, Jia R, Zhang HX, Bai FQ (2019) Effect of different topological structures (D-π-D and D-π-A-π-D) on the optoelectronic properties of benzo[2,1-B:3,4-B]dithiophene based donor molecules toward organic solar cells. Solar Energy 186:311–322. https://doi.org/10.1016/j.solener.2019.04.043

Boys SF, Bernardi F (2006) The calculation of small molecular interactions by the differences of separate total energies. Some procedures with reduced errors. Mol Phys 19:553–566. https://doi.org/10.1080/00268977000101561

Dong L, Hu S, Gao J (2020) Discovering drugs to treat coronavirus disease 2019 (COVID-19). Drug Discov Ther 14:58–60. https://doi.org/10.5582/ddt.2020.01012

Ergürhan O, Parlak C, Alver O, Şenyel M (2018) Conformational and electronic properties of hydroquinone adsorption on C60 fullerenes: doping atom, solvent and basis set effects. J Mol Struct 1167:227–231. https://doi.org/10.1016/j.molstruc.2018.04.092

Harapan H, Itoh N, Yufika A, Winardi A, Keam S, Te H, Megawati D, Hayati Z, Wagner AL, Mudatsir M (2020) Coronavirus disease 2019 (COVID-19): a literature review. J Infect Public Health 13:667–673. https://doi.org/10.1016/j.jiph.2020.03.019

Hazrati MK, Hadipour NL (2016a) Adsorption behavior of 5-fluorouracil on pristine, B-, Si-, and Al-doped C60 fullerenes: A first-principles study. Phys Lett A 380:937–941. https://doi.org/10.1016/j.physleta.2016.01.020

Hazrati MK, Hadipour NL (2016b) A DFT study on the functionalization of C60 fullerene with 1, 2-benzoquinone. Comput Theor Chem 1098:63–69. https://doi.org/10.1016/j.comptc.2016.11.007

Henna T, Raphey V, Sankar R, Shirin VA, Gangadharappa H, Pramod K (2020) Carbon nanostructures: the drug and the delivery system for brain disorders. Int J Pharm. https://doi.org/10.1016/j.ijpharm.2020.119701

Hiscott J, Alexandridi M, Muscolini M, Tassone E, Palermo E, Soultsioti M, Zevini A (2020) The global impact of the coronavirus pandemic. Cytokine Growth Factor Rev 53:1–9. https://doi.org/10.1016/j.cytogfr.2020.05.010

Huang H, Fan C, Li M, Nie HL, Wang FB, Wang H, Wang R, Xia J, Zheng X, Zuo X, Huang J (2020) COVID-19: a call for physical scientists and engineers. ACS Nano 14:3747–3754. https://doi.org/10.1021/acsnano.0c02618

Kazemzadeh H, Mozafari M (2019) Fullerene-based delivery systems. Drug Discovery Today 24:898–905. https://doi.org/10.1016/j.drudis.2019.01.013

Korotkikh N, Rayenko G, Saberov VS, Yenya V, Shvaika O (2019) The electronic properties of carbenes. J Organ Pharm Chem 17:28–36

Kumar M, Raza K (2017) C60-fullerenes as drug delivery carriers for anticancer agents: promises and hurdles. Pharm Nanotechnol 5:169–179. https://doi.org/10.2174/2211738505666170301142232

Liu M, Gao Y, Yuan Y, Yang K, Shi S, Zhang J, Tian J (2020) Efficacy and safety of integrated traditional chinese and western medicine for corona virus disease 2019 (COVID-19): a systematic review and meta-analysis. Pharmacol Res 158:104896. https://doi.org/10.1016/j.phrs.2020.104896

Maleki R, Khoshoei A, Ghasemy E, Rashidi A (2020) Molecular insight into the smart functionalized TMC-Fullerene nanocarrier in the pH-responsive adsorption and release of anti-cancer drugs. J Mol Graph Model 100:107660. https://doi.org/10.1016/j.jmgm.2020.107660

Novir SB, Aram MR (2020) Quantum mechanical simulation of Chloroquine drug interaction with C60 fullerene for treatment of COVID-19. Chem Phys Lett 757:137869. https://doi.org/10.1016/j.cplett.2020.137869

Parlak C, Alver O (2017) A density functional theory investigation on amantadine drug interaction with pristine and B, Al, Si, Ga, Ge doped C60 fullerenes. Chem Phys Lett 678:85–90. https://doi.org/10.1016/j.cplett.2017.04.025

Parlak C, Alver O, Şenyel M (2017) Computational study on favipiravir adsorption onto undoped- and silicon-decorated C60 fullerenes. J Theor Comput Chem 16:1750011. https://doi.org/10.1142/S0219633617500110

Parlak C, Tepe M, Bağlayan O, Alver O (2020) Investigation of detection and adsorption properties of β-propiolactone with silicon and aluminum doped fullerene C60 using density functional theory. J Mol Struct 1217:128346. https://doi.org/10.1016/j.molstruc.2020.128346

Patel R, Singh YP (2018) Synthesis, structural characterization, DFT studies and in-vitro antidiabetic activity of new mixed ligand oxovanadium (IV) complex with tridentate Schiff base. J Mol Struct 1153:162–169. https://doi.org/10.1016/j.molstruc.2017.10.010

Rad AS, Aghaei SM (2018) Potential of metal-fullerene hybrids as strong nanocarriers for cytosine and guanine nucleobases: a detailed DFT study. Curr Appl Phys 18:133–140. https://doi.org/10.1016/j.cap.2017.11.016

Rad AS, Ardjmand M, Esfahani MR, Khodashenas B (2020) DFT calculations towards the geometry optimization, electronic structure, infrared spectroscopy and UV-vis analyses of Favipiravir adsorption on the first-row transition metals doped fullerenes; a new strategy for COVID-19 therapy. Spectrochim Acta Part A Mol Biomol Spectrosc 247:119082. https://doi.org/10.1016/j.saa.2020.119082

Rad AS, Ardjmand M, Esfahani MR, Khodashenas B (2021) DFT calculations towards the geometry optimization, electronic structure, infrared spectroscopy and UV–vis analyses of Favipiravir adsorption on the first-row transition metals doped fullerenes; a new strategy for COVID-19 therapy. Spectrochim Acta Part A Mol Biomol Spectrosc 247:119082. https://doi.org/10.1016/j.saa.2020.119082

Raphey V, Henna T, Nivitha K, Mufeedha P, Sabu C, Pramod K (2019) Advanced biomedical applications of carbon nanotube. Mater Sci Eng, C 100:616–630. https://doi.org/10.1016/j.msec.2019.03.043

Reddy S, Lai WF (2021) Tackling COVID-19 using remdesivir and favipiravir as therapeutic options. Chembiochem 22:939–948

Samanta PN, Das KK (2017) Noncovalent interaction assisted fullerene for the transportation of some brain anticancer drugs: a theoretical

study. J Mol Graph Model 72:187–200. https://doi.org/10.1016/j.jmgm.2017.01.009
Shi J, Votruba AR, Farokhzad OC, Langer R (2010) Nanotechnology in drug delivery and tissue engineering: from discovery to applications. Nano Lett 10:3223–3230. https://doi.org/10.1021/nl102184c
Sissoko D, Laouenan C, Folkesson E, M'lebing AB, Beavogui AH, Baize S, Camara AM, Maes P, Shepherd S, Danel C (2016) Experimental treatment with favipiravir for Ebola virus disease (the JIKI Trial): a historically controlled, single-arm proof-of-concept trial in Guinea. PLoS medicine 13:e1001967. https://doi.org/10.1371/journal.pmed.1001967
Slepička P, Kasálková NS, Stránská E, Bačáková L, Švorčík V (2013) Surface characterization of plasma treated polymers for applications as biocompatible carriers. Express Polym Lett 7:535
Song Y, Liu P, Shi X, Chu Y, Zhang J, Xia J, Gao X, Qu T, Wang M (2020) SARS-CoV-2 induced diarrhoea as onset symptom in patient with COVID-19. Gut 69:1143–1144. https://doi.org/10.1136/gutjnl-2020-320891
Udwadia ZF, Singh P, Barkate H, Patil S, Rangwala S, Pendse A, Kadam J, Wu W, Caracta CF, Tandon M (2021) Efficacy and safety of favipiravir, an oral RNA-dependent RNA polymerase inhibitor, in mild-to-moderate COVID-19: a randomized, comparative, open-label, multicenter, phase 3 clinical trial. Int J Infect Dis 103:62–71. https://doi.org/10.1016/j.ijid.2020.11.142
Wu R, Wang L, Kuo HCD, Shannar A, Peter R, Chou PJ, Li S, Hudlikar R, Liu X, Liu Z, Poiani GJ, Amorosa L, Brunetti L, Kong AN (2020) An update on current therapeutic drugs treating COVID-19. Curr Pharmacol Rep 6:56–70
Zu ZY, Jiang MD, Xu PP, Chen W, Ni QQ, Lu GM, Zhang, (2020) Coronavirus disease 2019 (COVID-19): a perspective from China. Radiology 296:E15–E25. https://doi.org/10.1148/radiol.2020200490

Authors and Affiliations

Shamsa Bibi[1] · Shafiq Urrehman[1] · Laryeb Khalid[1] · Muhammad Yaseen[2] · Abdul Quyyam Khan[3] · Ran Jia[4]

✉ Shamsa Bibi
shamsa.shafiq@uaf.edu.pk

✉ Shafiq Urrehman
shafiq.urrehman@uaf.edu.pk

[1] Department of Chemistry, University of Agriculture Faisalabad, Faisalabad 38000, Pakistan

[2] Spin-Optoelectronics and Ferro-Thermoelectric (SOFT) Materials and Devices Laboratory, Department of Physics, University of Agriculture Faisalabad, Faisalabad 38000, Pakistan

[3] Pakistan Council of Scientific and Industrial Research Laboratories Complex, , Ferozepur Road, Lahore 54600, Pakistan

[4] Institute of Theoretical Chemistry and College of Chemistry, Jilin University, Changchun 130000, China